

The electrical surface potential of pulmonary surfactant

Zoya Leonenko^{1,2}, Matthias Amrein³

¹Department of Physics and Astronomy, ²Department of Biology, Faculty of Sciences, University of Waterloo, 200 University Avenue, West, Waterloo, N2L 3G1, Ontario, Canada; ³ Department of Cell Biology and Anatomy, Faculty of Medicine, University of Calgary, 3330 Hospital Drive NW, T2N 4N1, Alberta, Canada

TABLE OF CONTENTS

1. Abstract
2. Introduction
 - 2.1. Function and composition of pulmonary surfactant
 - 2.2. Structure of pulmonary surfactant
3. The Electric Surface Potential of Pulmonary Surfactant
 - 3.1. Measuring the electric surface potential
 - 3.2. The average surface potential
 - 3.3. Contrast in surface potential maps
4. The function of the surface potential
5. Summary and Perspective
6. Acknowledgment
7. References

1. ABSTRACT

A molecular film of pulmonary surfactant covers the hydrated lung epithelium to the air. We recently showed that the film exhibits a locally strongly variable electrical surface potential of up to several hundred millivolts. The potential arises from aligned molecular dipoles of the molecules. In the case of the complex structural organization of the phase-separated film of pulmonary surfactant, a map of the local surface potentials allows insight into the local distribution and order of its molecular constituents. Here, we summarize our recent findings and discuss how the electrical surface potential influences the architecture of the film but also changes the way how the lung interacts with the environment.

2. INTRODUCTION

2.1. Function and composition of pulmonary surfactant

Pulmonary surfactant forms a molecular film at the air-water interface of the hydrated air-alveolar interface. Surfactant is secreted by the alveolar type II epithelial cells as lamellar bodies (1, 2, 3). It evolves into tubular myelin and adsorbs to the air-water interface and forms a tightly packed molecular film. This film reduces the surface tension of a free air-water interface of about 70 mN/m to an equilibrium value of about 23 mN/m. As the area of the alveolar interface decreases upon expiration, the molecular film contracts and the surface tension drops further. Direct measurements in the lung revealed a surface tension of

Electrical surface potential of pulmonary surfactant

almost zero at residual lung capacity (4). During tidal breathing, it stayed well below 10 mN/m (5).

Phospholipids are the primary surface tension lowering components in surfactant. Phosphatidylcholines (PC) represent 80% of its mass. Half of the PC is the disaturated dipalmitoylphosphatidylcholine (DPPC); 5–10% by mass is the negatively charged phosphatidylglycerol (PG) (6). In a pure film, DPPC permits surface tension reduction to near zero values upon compression. A significant amount of phosphatidylglycerols (PG) or, in some cases, phosphatidylinositols (PI) suggests an important role for either one or both of these negatively charged phospholipids as well (7, 8). PG and PI have been shown to improve the adsorption of surfactant to the interface.

Pulmonary surfactant contains two water-soluble (SP-A, SP-D) and two hydrophobic surfactant-associated proteins (SP-B, SP-C). The latter two are permanently associated with the lipids of surfactant. Mixed films that also contain SP-C and/or SP-B can sustain a very low surface tension equally well as pure DPPC films. The proteins SP-C and -B efficiently recruit the lipids to the interface and promote more effective film organization. They are also responsible for the cohesiveness and mechanical strength of the film (8, 9, 10, 11, 12, 13, 14, 15, 16). Cholesterol is present with 5-10 % by mass (10-20 mol %) and constitutes the major fraction of the neutral lipids.

Lack of surfactant or dysfunctional surfactant is associated with high surface tension strongly impaired lung function. Pre-term infants do not have sufficient mature surfactant and as a result develop Respiratory Distress Syndrome (RDS) in a gestational age dependent manner. These neonates are treated by intra-tracheal administration of exogenous surfactant, spread from a bolus of a highly concentrated aqueous suspension. Notwithstanding the great success of this treatment, RDS remains one of the leading causes of the neonatal morbidity and mortality. In adult respiratory distress syndrome (ARDS), pulmonary surfactant is not lacking but functionally impaired. This coincides with an increase of cholesterol in surfactant to about 20% by weight or twice to four times its physiological level both in animals and humans (17, 18, 19, 20, 21, 22). We found for such an elevated level that cholesterol alone can fully account for the inhibition observed in ARDS, and the lowest surface tension observed by us was 16 mN/m (23).

2.2. Structure of pulmonary surfactant

The exceptional stability of functional surfactant and failure in case of disease is an active field of research (9, 23, 24, 25, 26, 39). In our recent studies, summarized in this review, we used lipid extract surfactant from bovine lung lavage (BLES). BLES is a surfactant representative of mammalian species and is currently used in hospitals as a surfactant replacement. It lacks the water soluble surfactant

proteins that play a minor role for surface activity. Cholesterol is removed from BLES during purification. We re-added cholesterol to some of the preparations to study its effects (23, 31, 32, 40, 41 and see also below).

For microscopy, the suspensions were spread at the air-buffer interface of a Langmuir trough into molecular films. After adjusting the area covered by the film until a defined surface tension was reached, the films were deposited on freshly cleaved ruby mica substrate using the Langmuir-Blodgett technique as described (31). Topographical images were collected in air with a NanoWizard™ AFM (JPK Instruments AG, Berlin), and surface potential maps were acquired as described below and in (31, 32).

Artificial or natural pulmonary surfactants that are functional in the sense that they can reduce the surface tension of an air-water interface close to zero show a pattern of bare monolayer and scattered multilayer regions on top of the monolayer (Figure 1, left) (9, 31, 42). Most of the time the height within stacks increases in increments of about 4 to 5 nm or multiples thereof. This is indicative that each layer consists of a lipid bilayer patch. For the films containing 20% cholesterol, stacks of multilayers or protrusions are missing almost entirely (Figure 1, right) (31, 40). The monolayer-bilayer conversion appears to be a well defined process with the involvement of either one or both hydrophobic surfactant associated proteins. This process is inhibited by excess of cholesterol and protrusions formed under this condition lack the defined protein-lipid complex structure of the functional films.

To understand, why bilayer stacks are required for function, they may be ascribed a mechanical role, similar to the role of reinforcing elements in preventing a thin plate from collapsing under lateral compression (43). In this analogy the surface tension is equivalent to an external lateral pressure compressing a plate and the molecular film is the continuum plate. The film will buckle above a critical compression. Buckling has been described as mode of failure for pulmonary surfactant (29). Qualitatively, having lipid bilayer patches on the surface breaks the large areas into smaller patches. According to the elastic theory, for a given cross section (or film thickness) the critical compression increases strongly with a decrease in size of the elements (43).

In order for the bilayer stacks to be mechanically reinforcing, they must be cross-linked to the monolayer. Otherwise, they will separate from- or glide over the monolayer area reduction and have no mechanical effect. Both hydrophobic proteins, SP-C and SP-B are likely acting as the cross-linkers (e.g. 9, 31, 44, 45, 46). In agreement with this proposed function, artificial or animal extract surfactants depend on the presence of either one or both hydrophobic proteins in order to lower the surface tension to a physiological low level. Cholesterol inhibits the monolayer-bilayer conversion and thus brings about failure of function.

Electrical surface potential of pulmonary surfactant

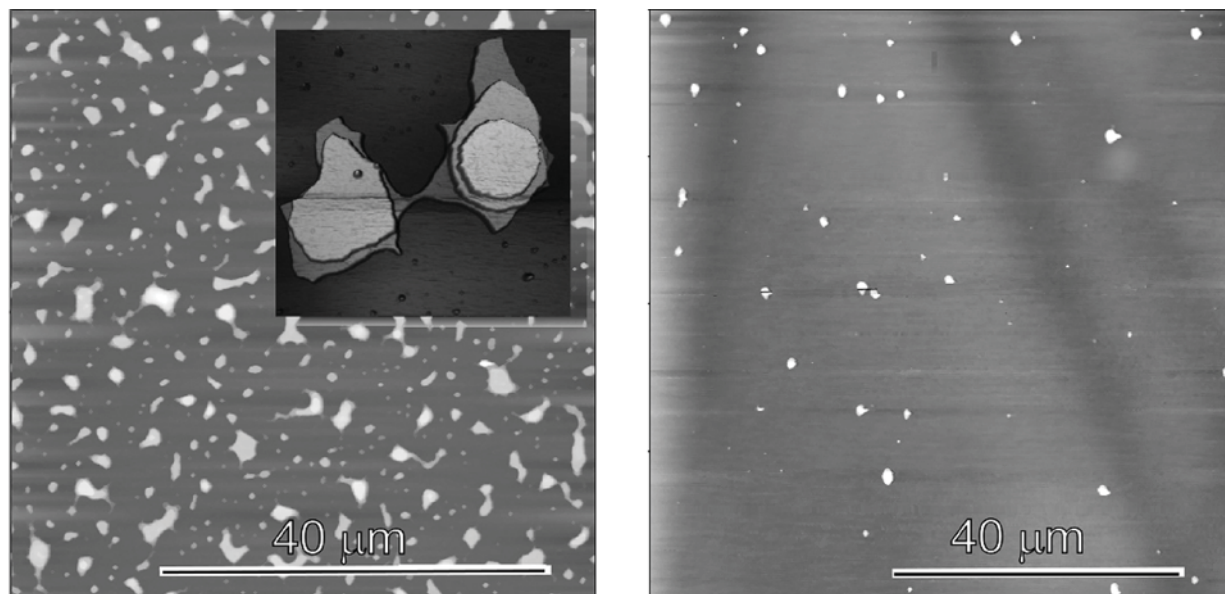


Figure 1. Reproduced with permission from Lanmuir. AFM topography of bovine lipid extract surfactant (BLES) films on mica with 5% (left) and 20% cholesterol by weight (right). Topographical height is displayed in levels of gray with lower regions being darker. The topography of BLES films with 0% is similar to 5% cholesterol (not shown). The films were formed at the air-water interface of a Langmuir trough and the area reduced until a film pressure of 47 mN/m was reached (corresponding to a surface tension of 26 mN/m). For the microscopy, the films were transferred onto a mica support by the Langmuir-Blodgett technique. For both conditions, the entire interface is covered by at least one monolayer of lipids (dark gray background). Bright patches are stacks of lipid bilayers on top of the monolayer as indicated by a prevalent step height of about 4 to 5 nm. The insert in Fig 1, left, is a pseudo three-dimensional representation (size 2.5 μm by 2.5 μm). Multilamellar structures are mostly absent in the film on the right. Reproduced with permission from 41.

3. THE ELECTRIC SURFACE POTENTIAL OF PULMONARY SURFACTANT

3.1. Measuring the electric surface potential

In 1861, the Scottish scientist Lord Kelvin introduced the Kelvin Probe method, to obtain an averaged (spatially not resolved) measure of the potential of interfaces (47). The Kelvin Probe method is a non-contact, non-destructive method to investigate properties of materials. Kelvin-Probe Force microscopy extends this principle to map the local surface potential with high spatial resolution rather than just globally measure the average potential of a film. Kelvin probe force microscopy (KPFM) is a scanning probe technique capable of mapping the local surface potential or surface charge distribution with spatial resolution. KPFM, also known as surface potential microscopy, is a noncontact atomic force microscopy (AFM), in which the electrostatic interaction is minimized by application of an appropriate bias voltage during imaging topographic imaging using the same principle as a macroscopic Kelvin probe method. With KPFM, the work function or surface potential can be resolved with lateral resolution at nm scale (48, 29, 50, 51). To date, KPFM on organic films has been successfully used to study amphiphilic molecules, and a biological membrane (52, 53, 54, 55). KPFM is designed to map the surface potential of an interface to the air or vacuum. KPFM is therefore particularly well suited to investigate pulmonary

surfactant films that physiologically occur at the lung's interface to the air. Most macromolecular, biological systems reside in an aqueous environment, however. There local surface charge distribution may be explored by a method, related to KPFM (56).

In our studies, two different implementations of this scheme were used (31, 41). In one method AFM topography was on the scanning trace, and on the retrace the probe was lifted and scanned around 50 nm above the sample surface (Figure 2). During the Kelvin scan (retrace) superimposed dc voltage and ac voltages were applied between the probe and the sample. In this approach when the probe interacts with the sample surface and feels electrostatic interaction, the probe starts oscillating mechanically. To nullify this mechanical oscillation and the electrostatic forces, which cause it, additional dc voltage is applied to the probe, which gives the measure of changes in the surface potential during the scan (57).

The other method allows for simultaneous collection of AFM topography and KPFM images (Figure 4). This method is called Frequency Modulated Kelvin Probe Force Microscopy (FM-KPFM) and was recently developed in the group of Dr. L. Eng, sample (48, 49, 50). This method allows simultaneous recording of topographic and local surface potential images with high resolution and high sensitivity, and is not affected by the sharpness of the

Electrical surface potential of pulmonary surfactant

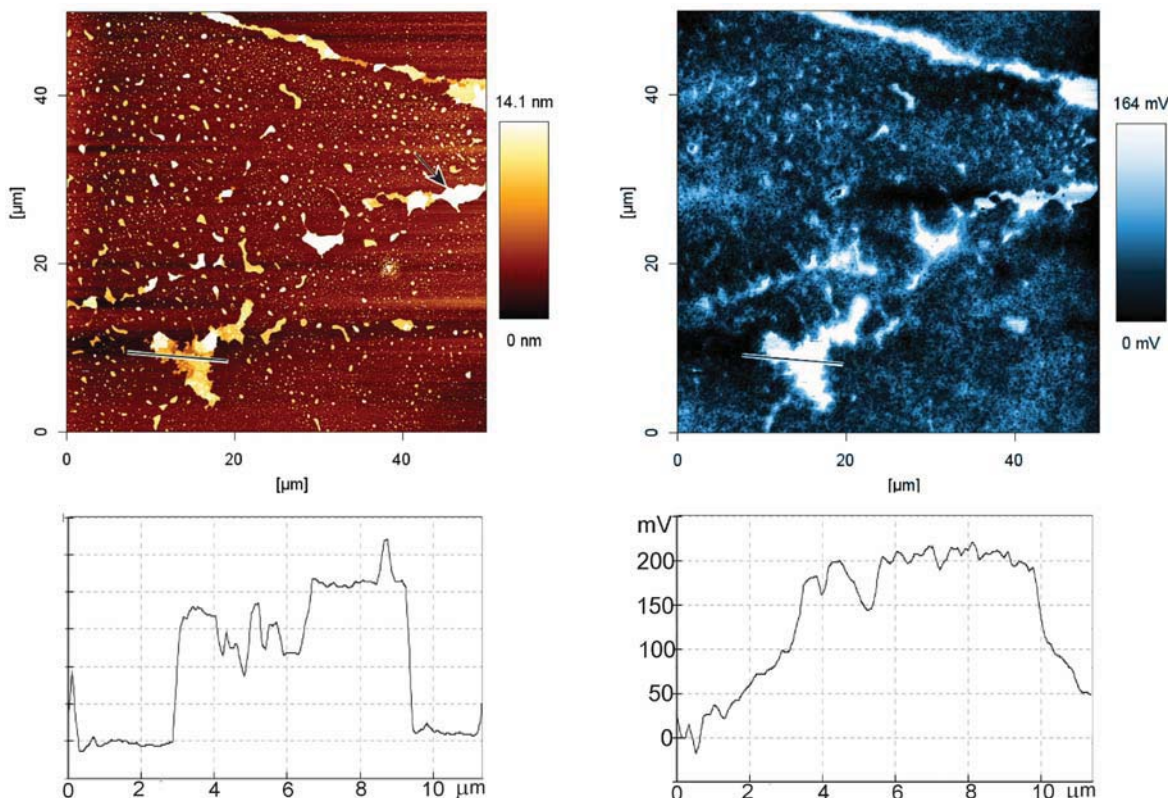


Figure 2. Overview of a film of BLES that contains no cholesterol. The topographical image (left, cross section below) shows the above described (Figure 1) pattern of monolayer (dark brown) and scattered multilayer regions (brighter colors). In the potential map (right and cross section below) large stacks of bilayer patches are at a potential of up to 200 mV above the monolayer. Brighter hues indicate a more positive surface potential with respect to darker hues) The arrows in the topographical image and in the potential map point to a region, where the topographical height does not change but the potential shows two distinct levels. Reproduced with permission from 31.

probe or the distance from the sample. The FM-KPFM technique is based on frequency modulation, which is measured during the scan, instead of amplitude modulation as described above.

Both methods revealed similar potentials for corresponding film areas (31, 41). From this, we conclude that mapping the electrical surface potential of pulmonary surfactant is reliable and reproducible. KPFM also proves to be a high resolution microscopy for the surfactant films. The potential map shows structures as small as about 50 nm (Figure 4). This may indeed reflect the smallest electrical domains in these films, and the highest resolution offered by KPFM has been shown to be better than 50 nm (48, 57). A high signal to noise ratio in the potential maps allows distinguishing electrical domains in an unambiguous manner. The dynamic range of the potential for all maps shown in this review exceeds 100 mV and is thus at least two orders of magnitude larger than the minimum difference in potential that can be resolved by our instruments (48).

3.2. The average surface potential

Lipid films at an air-water interface exhibit an electrical surface potential. The potential is a function of

the strength of the molecular dipoles in direction perpendicular to the interface μ , the dielectric constant ϵ and the packing density or area, covered by each molecule A . For phospholipids, contributions have been ascribed to various regions of the molecules, each in its own dielectric environment; the head-group region, the aliphatic tail and the terminal methyl group (58). Hydration and, hence, a high dielectric constant in this region, will make the contribution of the head group to the overall surface potential small (58).

$$V = \frac{1}{A\epsilon_0} \left[\frac{\mu_1}{\epsilon_1} + \frac{\mu_2}{\epsilon_2} + \frac{\mu_3}{\epsilon_3} \right]$$

Note that a free air-water interface exhibits a surface potential too, because of an alignment of water molecules at the interface (59). However, at surface tensions as low as used in the reviewed studies, the interface is fully covered by the surfactant molecules with no residual free air-water interface.

The average surface potential found in our recent studies may be compared to the reported surface potential obtained by the Kelvin method. Surprisingly, we found a

Electrical surface potential of pulmonary surfactant

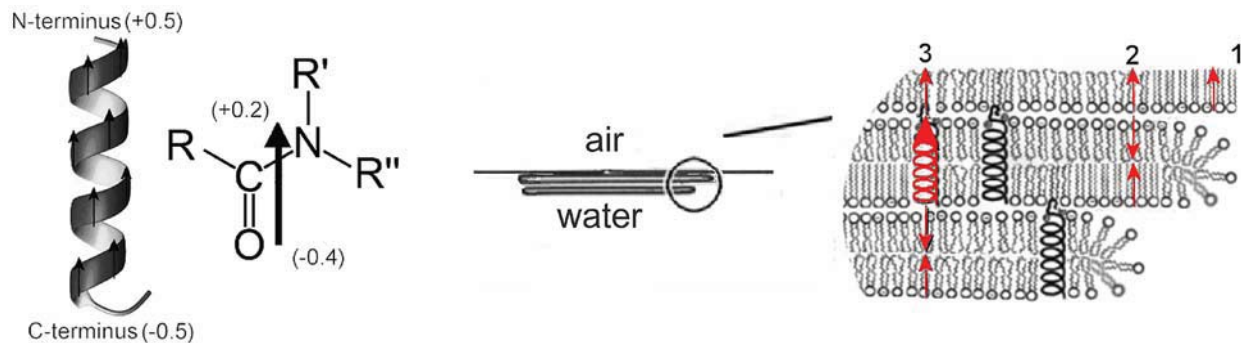


Figure 3. left: Alpha-helices are distinct by a molecular dipole moment in direction of the helix axis. This is because of the aligned molecular dipole posed by the amide bond (numbers are in fractions of unit charge). The dipole sums up to about one half of a unit charge on each side times the length of the helix. right: The molecular architecture of pulmonary surfactant. 1, 2 and 3 denote three situations of arrangement of molecular dipoles. The molecular arrangement of pulmonary surfactant films should lead to a positive surface potential in monolayer regions (denoted by 1), a potential similar to the monolayer region if a monolayer region is covered by lipid bilayer patches devoid of protein (2) and a region of a more strongly positive surface potential over bilayer patches that contain SP-C (3). The arrows in figure 4A and B depict the molecular dipole moment, pointing to the positive pole. The dipole of SP-C in figure 4 B is depicted with an arrowhead and a helical tail.

negative average surface potential found for all films investigated (approximately $-0.5V$, depending on the film). Films of dipalmitoyl phosphatidyl choline (DPPC), the most abundant of the surfactant components (approximately 40% by weight), has been reported by most authors to give rise to an overall surface potential of about $+0.5V$, when compressed to a surface pressure of about 40 mN/m at the air-water interface (60). An overriding negative contribution of surfactant components other than DPPC offers no plausible explanation for this discrepancy because the overall surface potential of pulmonary surfactant films is comparable to pure DPPC films (personal communication, Manfred Sieber). However, Mozaffary reported a negative sign of the surface potential similar to what we found here (59). They explain the differences in sign in terms of the different reference points, or ground, used in different studies. Moreover, the electrical potential V_{app} measured in the current study may carry an offset to the true surface potential ϕ . This is because the electrical potential is not only caused by the surface potential ϕ , itself, but also an additional potential difference between the probe and the substrate, V_{CPD} :

$$V_{app} = V_{CPD} + \phi.$$

It is difficult to estimate the absolute numbers for V_{CPD} and ϕ separately and an uncertainty therefore remains with respect to an offset of the electrical potential for our findings. Measuring V_{CPD} and ϕ for the mica support alone will not likely return a meaningful measure for such offset because bare mica is coated by a water film in an ambient environment and, hence, presents a very different interface from mica underneath the surfactant film.

There may be another difference between the surface potential of a film at the air-water interface and the films investigated here because of deposition of the latter

onto a solid support. While we have shown earlier that the overall structure of the film is not affected by the transfer, the head group may be at least partially dehydrated (44). This may increase the contribution of the head group to the overall surface potential.

Owing to the uncertainty about the absolute surface potential of the surfactant films, we used a relative scale for the display of the spatial potential distribution map in figure 2. Such relative values of the potential within a mapped area are not affected by the difficulty with determining the absolute potential of a film. Moreover, for identical experimental conditions, assuming that all contributions from the substrate and the probe are the same, one may also compare one sample to another (54). We found the surface potential of films containing 0% or 5% cholesterol to be more negative ($-0.6V$) than films containing 20% cholesterol ($-0.4V$). This is in accordance with earlier findings that cholesterol decreases the electric potential of DPPC monolayer (59).

3.3. Contrast in surface potential maps

Segregation of molecular components and the specific molecular arrangement gives rise to the locally variable surface potential. The most striking feature in the surface potential maps of functional pulmonary surfactant is the positive (or less negative) regions ($+0.2 \pm 0.05 V$), where in the topography there are stacks of lipid bilayers adjacent to the monolayer. It is expected that a strong surface potential arises from surfactant associated protein C (SP-C). SP-C is a small (molecular mass $\sim 4 \text{ kDa}$) hydrophobic protein with a membrane spanning alpha-helical segment (61, 62). Two palmitoyl-groups are covalently linked to the two cysteine residues located in the N-terminal region. We have shown that SP-C promotes the formation of lipid bilayer patches and resides in these multilamellar regions of the surfactant films (63). The most likely arrangement of SP-C in the lamellar region is with its helical axis perpendicular to the interface (discussed in 15). SP-C possesses a particularly strong molecular dipole

Electrical surface potential of pulmonary surfactant

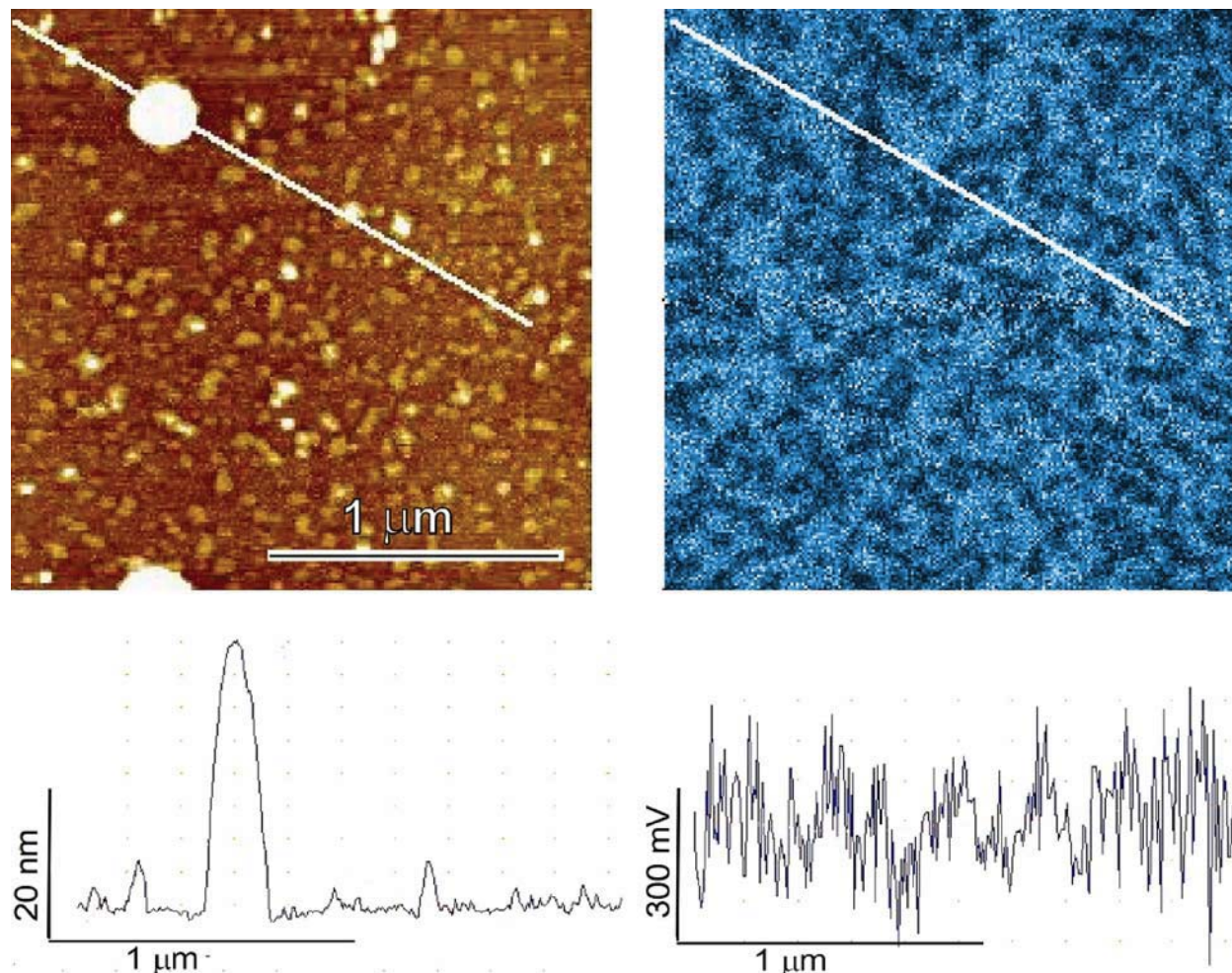


Figure 4. AFM topography (left) and surface potential map (right) of a dysfunctional surfactant film (BLES with 20% cholesterol, surface pressure 47 mN/m). Cross-sections as indicated in the images are displayed under the bottom row of images. Large lipid aggregates seen in the topographical image are electrically transparent. The monolayer area shows a structured surface potential. Small domains are also visible in the high resolution topographical image.

moment in direction of its molecular axis due to its α -helical secondary structure and because of the positive charges near its N-terminal. If arranged with its N-terminal pointing towards the air, this should effectively induce a more positive surface potential in the multi-layered areas of the film and thus explain the more positive surface potential found on the multi-layered regions (Figure 3).

It is notable that the other known hydrophobic surfactant associated protein, SP-B, is also present in BLES and also promotes the formation of lamellar structures (9, 64). SP-B is a member of the saposin-like family of peptides (molecular mass 17 kDa) (65, 66). The tertiary structure may closely resemble NK-lysin because of the high similarity (67). There appear to be five amphipatic helices (i.e. the helices are distinguished by a highly hydrophobic face on the one side and a hydrophilic face on the opposite side of the helix-axis). These helices have been

proposed to be aligned partially immersed in the lipid layer with the axis parallel to the interface. Since in the compressed film the molecular dipoles of the helices should also be mostly parallel to the interface, they should not contribute to the surface potential.

Some regions may consist of lipid bilayers, devoid of protein. Bilayers devoid of protein should be electrically “transparent” as the molecular dipoles from the lower and the upper leaflet are of opposite direction and, as a result, their contribution to the surface potential cancel out. We showed earlier by scanning near-field optical microscopy that multi-layered regions with and without SP-C may indeed co-exist.

When 20% cholesterol was present in the BLES film, there were not many multilayer structures, but occasional spherical aggregates (Figure 4, left). These structures were transparent in the electrical potential image

Electrical surface potential of pulmonary surfactant

(Figure 4, right). The absence of a contrast in the Kelvin signal in this case may reflect a disordered molecular arrangement where molecular dipoles cancel out.

Another aspect of the molecular arrangement becomes evident in the monolayer area of the surfactant films. For films that contain no cholesterol the monolayer areas are neither structured in topography nor the potential map. In contrast, films containing cholesterol are strongly structured in the potential image (± 0.2 V, Figure 4, right)). It has been shown by fluorescence light microscopy (e.g. 68-71), that surfactant containing no cholesterol segregates into large condensed domains, whereas cholesterol containing surfactants no longer show this phase pattern of micrometer dimensions in light microscope (70, 71). However, our surface potential maps reveal that the molecular components in these films still segregate, but form domains of a size not resolved in a light microscope. In analogy, cholesterol is known to condense saturated lipid species of the plasma membrane into nano-scaled domains (sphingolipid-cholesterol rafts). Because cholesterol promotes a more positive surface potential in phospholipid films, one could assume that the brighter areas in the monolayer contain the cholesterol.

In summary, mapping the electrical surface potential allowed us to propose a molecular arrangement of the constituents of pulmonary surfactant films with great detail. More studies are now required to provide firm proof for the proposed molecular detail of the film architecture. For example, films devoid of either SP-C or SP-B or both will have to be compared to current data. Lack of certainty about the absolute surface potential or the influence of head group dehydration during film deposition can only be addressed by carrying out the KPFM microscopy on films directly at the air-water interface. Pulmonary surfactant films have been imaged by AFM directly at the air-water interface by approaching the interface by an AFM tip submerged in the aqueous subphase (72). Approaching the interface from the air by an AFM tip may prove more difficult. Small airborne particles have been shown to adhere to surfactant and become submerged, a fate that may be shared by the AFM tip (73).

Despite the difficulties still associated with KPFM of pulmonary surfactant, the method holds great potential. The electrical surface potential is a signature of the molecules and their arrangement themselves. This is important for a structure where labeling such as for fluorescence light microscopy so far mostly allowed for a mere distinction between a more ordered and a less ordered phase. Moreover, the surface potential in the case of pulmonary surfactant may be of great consequence how the film assembles into its defined structure, but also how the lung interacts with inhaled nanoparticles. This is discussed in the next section.

4. THE FUNCTION OF THE SURFACE POTENTIAL

We so far discussed the surface potential maps as a means to study molecular architecture of the surfactant films. However, the surface potential itself may play a role

in defining the molecular architecture. Formation and size of domains in interfacial films of surfactants are governed by the tension of the domain boundary from a surrounding matrix on one hand and the stress caused by an electrical surface potential within a single domain on the other hand (e.g. 74). A high surface potential causes domains to become dispersed and small, while high boundary tension promotes formation of large domains. Cholesterol in mixed films of phospholipids and related molecules is known to reduce the boundary tension (71, 75). The absence of a high boundary tension in BLES containing cholesterol may therefore explain the formation of the small domains. Our observation correlates with the effect of lipid condensation in small domains, produced by cholesterol, reported earlier (e.g. 59, 71), but in addition shows that these domains differ in the electric potential.

Another important function of the surface potential relates to the interaction of airborne particles, entering the lung. Both man-made and natural particles are invariably electrically charged, and their fate in the lung is also influenced by this electrical charge (76). The movement of small particles ($< 0.5\mu\text{m}$) in the lung has largely been described to be by diffusion and chaotic mixing (77, 78, 79). However, these small particles will also be affected strongly by electrostatic attraction. Bailey *et al.* have shown that moderately charged particles ($q=200$ electrons) with a diameter of $0.5\mu\text{m}$ are deposited in the alveolar lung about five times as efficiently as uncharged particles. Until now, any electrostatic interaction of particles with the alveolar wall has been ascribed to the attraction of an electrical charged particle and its electrical image induced in the alveolar wall. We now offer an additional mechanism for this behavior; the interaction of the charged particles with the electrical field arising from the surface potential of the surfactant film. Note that in a conductive sphere, no electrical field would be expected in the interior and an alveolus should behave like a sphere. Unlike a conductor, however, the charges or molecular dipoles at the alveolar-air interface are not free to move and the interface is not homogeneously charged inside the alveoli. Thus, different domains act as electrical poles and give rise to an electrical field. Local field strength depends on both the lateral distribution and potential difference between the local electrical poles. We currently evaluate theoretically, using actual surface potential maps, and experimentally, using force spectroscopy, how the electrical surface potential landscape of pulmonary surfactant interferes with the amount of particle deposition in the lung as well as how local variations in the electric potential defines a distinctive affinity of particles to one region of the surfactant film over other areas.

5. SUMMARY AND PERSPECTIVE

In summary, functional and dysfunctional pulmonary surfactant films show distinctly different surface potential landscapes. Evaluating the surface potential maps by KPFM has contributed to identifying the molecular architecture related to function and understanding failure. The potential maps suggest that the interaction of airborne particles with the lung's walls needs to be re-evaluated taking the electrostatic interaction into account.

6. ACKNOWLEDGMENT

The current work was supported by the Canadian Institute for Health Research and the Canadian Foundation for Innovation. We thank Dr. Elmar Prenner for giving us access to a Langmuir trough, Dr. Robert French and Dr. W. Michael Schoel for critical reading of this manuscript.

7. REFERENCES

1. A. D. Bangham, C. J. Morley and M. C. Phillips: The physical properties of an effective lung surfactant, *Biochim Biophys Acta* 573, 552-556 (1979)
2. E. S. Brown, Isolation and Assay of Dipalmityl Lecithin in Lung Extracts, *Am J Physiol* 207, 402-406 (1964)
3. R. H. Notter, Lung Surfactants: Basic Science and Clinical Applications. *Marcel Dekker*, 2000.
4. S. Schurch, Surface tension at low lung volumes: dependence on time and alveolar size, *Respir Physiol* 48, 339-55. (1982)
5. H. Bachofen and S. Schurch: Alveolar surface forces and lung architecture, *Comparative Biochemistry and Physiology*, 183-193 (2001)
6. S. A. Shelley, J. U. Balis, J. E. Paciga, C. G. Espinoza and A. V. Richman: Biochemical composition of adult human lung surfactant, *Lung* 160, 195-206. (1982)
7. R. Veldhuizen, K. Nag, S. Orgeig and F. Possmayer: The role of lipids in pulmonary surfactant, *Biochim Biophys Acta-Mol Basis Dis* 1408, 90-108 (1998)
8. E. J. Veldhuizen, J. J. Batenburg, L. M. Van Golde and H. P. Haagsman: The role of surfactant proteins in DPPC enrichment of surface films, *Biophys. J.* 79, 3164 (2000)
9. M. M. Lipp, K. Y. C. Lee, D. Y. Takamoto, J. A. Zasadzinski and A. J. Waring: Coexistence of buckled and flat monolayers, *Phys Rev Lett* 81, 1650-1653 (1998)
10. K. Nag, J. Perez-Gil, A. Cruz, N. H. Rich and K. M. Keough: Spontaneous formation of interfacial lipid-protein monolayers during adsorption from vesicles, *Biophys J* 71, 1356-63. (1996)
11. S. G. Taneva and K. M. W. Keough: Pulmonary surfactant proteins SP-B and SP-C in spread monolayers at the air-water interface: I. Monolayers of pulmonary surfactant protein SP-B and phospholipids. *Biophys. J.* 66, 1137-1148 (1994)
12. S. G. Taneva and K. M. W. Keough: Pulmonary surfactant proteins SP-B and SP-C in spread monolayers at the air-water interface: II. Monolayers of pulmonary surfactant protein SP-C and phospholipids, *Biophys. J.* 66, 1149-1157 (1994)
13. T. E. Weaver and J. J. Conkright: Function of surfactant proteins b and c, *Annu Rev Physiol* 63, 555-78. (2001)
14. J. Perez-Gil, K. Nag, S. Taneva and K. M. Keough: Pulmonary surfactant protein SP-C causes packing rearrangements of dipalmitoylphosphatidylcholine in spread monolayers, *Biophys J* 63, 197-204. (1992)
15. M. Amrein, A. von Nahmen and M. Sieber: A scanning force- and fluorescence light microscopy study of the structure and function of a model pulmonary surfactant, *Eur Biophys J* 26, 349-57. (1997)
16. M. Gustafsson, M. Palmblad, T. Curstedt, J. Johansson and S. Schurch: Palmitoylation of a pulmonary surfactant protein C analogue affects the surface associated lipid reservoir and film stability, *Biochim Biophys Acta* 1466, 169-78. (2000)
17. S. A. Shelley, Oxidant-induced alterations of lung surfactant system, *J Fla Med Assoc* 81, 49-51 (1994)
18. A. Panda K., K. Nag, R. Harbottle R., K. Rodriguez-Capote, R. Veldhuizen A.W., N. Petersen O. and F. Possmayer: Effect of Acute Lung Injury on Structure and Function of Pulmonary Surfactant Films, *Am. J. Respir. Cell Mol. Biol.* 30, 641-650 (2004)
19. P. R. Rocco and W. A. Zin: Pulmonary and extrapulmonary acute respiratory distress syndrome: are they different? *Curr Opin Crit Care* 11, 10-7 (2005)
20. K. G. Davidson, A. D. Bersten, H. A. Barr, K. D. Dowling, T. E. Nicholas and I. R. Doyle: Lung function, permeability, and surfactant composition in oleic acid-induced acute lung injury in rats, *Am J Physiol -Lung Cell Mol Physiol* 279, L1091-L1102 (2000)
21. R. Schmidt, C. Ruppert, P. Markart, N. Lubke, L. Ermert, N. Weissmann, A. Breithecker, M. Ermert, W. Seeger and A. Gunther: Changes in pulmonary surfactant function and composition in bleomycin-induced pneumonitis and fibrosis, *Toxicol Appl Pharmacol* 195, 218-31 (2004)
22. G. Karagiorga, G. Nakos, E. Galiatsou and M. E. Lekka: Biochemical parameters of bronchoalveolar lavage fluid in fat embolism, *Intensive Care Med* 32, 116-123 (2006)
23. L. Gunasekara, S. Schurch, W. M. Schoel, K. Nag, Z. Leonenko, M. Haufs and M. Amrein: Pulmonary surfactant function is abolished by an elevated proportion of cholesterol, *Biochimica Et Biophysica Acta* 1737, 27-35 (2005)
24. M. K. Ratajczak, C. Jiarpinitnun, A. J. Waring and K. Y. C. Lee: Biophysical characterization of lung surfactant protein B and its mutant engineered peptides, *Biophysical Journal* 86, 374A-374A (2004)

Electrical surface potential of pulmonary surfactant

25. A. Gopall, H. Diamant, T. A. Witten and K. Y. C. Lee: Folding in model lung surfactant monolayers, *Biophysical Journal* 84, 510A-510A (2003)
26. H. Diamant, T. A. Witten, K. Y. C. Lee, A. Gopal and C. Ege: Topography and instability of model lung surfactant monolayers, *Biophysical Journal* 82, 547A-548A (2002)
27. A. Gopal, A. Waring and K. Y. C. Lee: Lung surfactant peptide SP-B1-25 and collapse transitions in phospholipid monolayers, *Biophysical Journal* 82, 144A-144A (2002)
28. A. Gopal, A. J. Waring and K. Y. C. Lee: How do lung surfactant peptides affect 2-D/3-D transitions in lipid monolayers? *Abstracts Of Papers Of The American Chemical Society* 222, U118-U118 (2001)
29. A. Gopal and K. Y. C. Lee: Morphology and collapse transitions in binary phospholipid monolayers, *J Phys Chem B* 105, 10348-10354 (2001)
30. K. Y. C. Lee, M. M. Lipp, D. Y. Takamoto, J. A. Zasadzinski and A. J. Waring: Collapse mechanism in lung surfactant system, *Abstr Pap Am Chem Soc* 216, 288-COLL (1998)
31. Z. Leonenko, S. Gill, S. Baoukina, L. Monticelli, J. Doehner, L. Gunasekara, F. Felderer, M. Rodenstein, L. M. Eng and M. Amrein: An elevated level of cholesterol impairs self-assembly of pulmonary surfactant into a functional film, *Biophys J* 93, 674-83 (2007)
32. Z. Leonenko, E. Finot, V. V and M. Amrein: Effect of cholesterol on the physical properties of pulmonary surfactant films: atomic force measurements study, *Ultramicroscopy* 106, 687-94 (2006)
33. S. Baoukina, L. Monticelli, M. W. Amrein and D. P. Tieleman: The molecular mechanism of monolayer-bilayer transformations of lung surfactant from molecular dynamics simulations, *Biophys J BioFAST* (2007). 10.1529/biophysj.107.113399
34. H. Nakahara, S. Lee, G. Sugihara and O. Shibata: Mode of interaction of hydrophobic amphiphilic alpha-helical peptide/dipalmitoylphosphatidylcholine with phosphatidylglycerol or palmitic acid at the air-water interface, *Langmuir* 22, 5792-5803 (2006)
35. C. Alonso, A. Waring and J. A. Zasadzinski: Keeping lung surfactant where it belongs: Protein regulation of two-dimensional viscosity, *Biophysical Journal* 89, 266-273 (2005)
36. C. Alonso, T. Alig, J. Yoon, F. Bringezu, H. Warriner and J. A. Zasadzinski: More than a monolayer: Relating lung surfactant structure and mechanics to composition, *Biophys J* 87, 4188-4202 (2004)
37. N. Biswas, S. Shanmukh, A. J. Waring, F. Walther, Z. D. Wang, Y. Chang, R. H. Notter and R. A. Dluhy: Structure and properties of phospholipid-peptide monolayers containing monomeric SP-B1-25 - I. Phases and morphology by epifluorescence microscopy, *Biophysical Chemistry* 113, 223-232 (2005)
38. D. Y. Takamoto, M. M. Lipp, A. von Nahmen, K. Y. C. Lee, A. J. Waring and J. A. Zasadzinski: Interaction of lung surfactant proteins with anionic phospholipids, *Biophys J* 81, 153-169 (2001)
39. J. Q. Ding, D. Y. Takamoto, A. von Nahmen, M. M. Lipp, K. Y. C. Lee, A. J. Waring and J. A. Zasadzinski: Effects of lung surfactant proteins, SP-B and SP-C, and palmitic acid on monolayer stability, *Biophys J* 80, 2262-2272 (2001)
40. L. Gunasekara, W. M. Schoel, S. Schürch and M. W. Amrein: A comparative study of mechanisms of surfactant inhibition, *BBA-Biomembranes* 1778, 433-444 (2008)
41. Z. Leonenko, M. Rodenstein, J. Dohner, L. M. Eng and M. Amrein: Electrical surface potential of pulmonary surfactant, *Langmuir* 22, 10135-9 (2006)
42. S. Baoukina, L. Monticelli, M. Amrein and D. P. Tieleman: The molecular mechanism of monolayer-bilayer transformations of lung surfactant from molecular dynamics simulations, *Biophys J* 93, 3775-3782 (2007). 10.1529/biophysj.107.113399
43. S. K. Fenster and A. C. Ugural: *Advanced Strength and Applied Elasticity*. New Jersey: Prentice Hall, 2003.
44. A. Nahmen von, M. Schenk, M. Sieber and M. Amrein: The Structure of a Model Pulmonary Surfactant as Revealed by Scanning Force Microscopy, *Biophys. J.* 72, 463-469 (1997)
45. W. Zisman, The Effect of Pressure on the Electrical Conductance of Salt Solutions in Water, *Physical Review* 39, 151-160 (1932)
46. W. Zisman, A NEW METHOD OF MEASURING CONTACT POTENTIAL DIFFERENCES IN METALS, *Rev Sci Instrum* 3, 367 (2004)
47. Lord Kelvin, Contact electricity of metals, *Philos Mag* 46, 82-120 (1898)
48. U. Zerweck, C. Loppacher, T. Otto, S. Grafstrom and L. M. Eng: Accuracy and resolution limits of Kelvin probe force microscopy, *Phys Rev B* 71, 125424-125433 (2005)
49. M. Fujihira, Kelvin Probe Force Microscopy of Molecular Surfaces, *Annual Reviews in Materials Science* 29, 353-380 (1999)
50. S. Kitamura, K. Suzuki and M. Iwatsuki: High resolution imaging of contact potential difference using a novel ultrahigh vacuum non-contact atomic force microscope technique, *Appl Surf Sci* 140, 265-270 (1999)

Electrical surface potential of pulmonary surfactant

51. R. Lüthi, E. Meyer, M. Bammerlin, A. Baratoff, T. Lehmann, L. Howald, C. Gerber and H. J. Güntherodt: Atomic resolution in dynamic force microscopy across steps on Si (1 1 1) 7×7 , *Zeitschrift für Physik B Condensed Matter* 100, 165-167 (1996)
52. L. F. Chi, S. Jacobi and H. Fuchs: Chemical identification of differing amphiphiles in mixed Langmuir-Blodgett films by scanning surface potential microscopy, *Thin Solid Films* 284-285, 403-407 (1996)
53. S. Jacobi, L. F. Chi and H. Fuchs: Combined scanning force, lateral force, and scanning surface potential microscopy on phase separated Langmuir-Blodgett films, *J. Vac. Sci. Technol. B* 14, 1503-1508 (1996)
54. J. Lu, E. Delamarche, L. Eng, R. Bennewitz, E. Meyer and H. J. Güntherodt: Kelvin probe force microscopy on surfaces: Investigation of the surface potential of self-assembled monolayers on gold, *Langmuir* 15, 8184-8188 (1999)
55. H. F. Knapp, P. Mesquida and A. Stemmer: Imaging the surface potential of active purple membrane, *Surf Interface Anal* 33, 108-112 (2002)
56. A. S. Johnson, C. L. Nehl, M. G. Mason and J. H. Hafner: Fluid electric force microscopy for charge density mapping in biological systems, *Langmuir* 19, 10007-10010 (2003)
57. M. Nonnenmacher, M. P. Oboyle and H. K. Wickramasinghe: Kelvin Probe Force Microscopy, *Appl Phys Lett* 58, 2921-2923 (1991)
58. P. Dynarowicz-Latka, A. Dhanabalan and O. N. Oliveira Jr.: Modern physicochemical research on Langmuir monolayers, *Advances in Colloid and Interface Science* 91, 221-293 (2001)
59. H. Mozaffary, On the sign and origin of the surface potential of phospholipid monolayers, *Chem Phys Lipids* 59, 39-47 (1991)
60. H. Brockman, Dipole potential of lipid membranes, *Chem. Phys. Lipids* 73, 57-79 (1994)
61. J. Johansson, T. Szyperski and K. Wüthrich: Pulmonary surfactant-associated polypeptide SP-C in lipid micelles: CD studies of intact SP-C and NMR secondary structure determination of dipalmitoyl-SP-C (1-17), *FEBS Lett.* 362, 261-265 (1995)
62. J. Johansson, T. Curstedt and B. Robertson: The proteins of the surfactant system, *Eur. Respir. J.* 7, 372-391 (1994)
63. A. Kramer, A. Wintergalen, M. Sieber, H. J. Galla, M. Amrein and R. Guckenberger: Distribution of the surfactant-associated protein C within a lung surfactant model film investigated by near-field optical microscopy, *Biophys J* 78, 458-65. (2000)
64. S. Krol, M. Ross, M. Sieber, S. Kunneke, H. J. Galla and A. Janshoff: Formation of three-dimensional protein-lipid aggregates in monolayer films induced by surfactant protein B, *Biophys J* 79, 904-18. (2000)
65. L. Patthy, Homology of the precursor of pulmonary surfactant-associated protein SP-B with prosaposin and sulfated glycoprotein 1, *J Biol Chem* 266, 6035-7. (1991)
66. S. Hawgood, M. Derrick and F. Poulain: Structure and properties of surfactant protein B, *Biochim Biophys Acta* 1408, 150-60. (1998)
67. M. Andersson, T. Curstedt, H. Jornvall and J. Johansson: An amphipathic helical motif common to tumourolytic polypeptide NK-lysin and pulmonary surfactant polypeptide SP-B, *FEBS Lett* 362, 328-32. (1995)
68. A. Post, A. V. Nahmen, M. Schmitt, J. Ruths, H. Riegler, M. Sieber and H. J. Galla: Pulmonary surfactant protein C containing lipid films at the air-water interface as a model for the surface of lung alveoli, *Mol Membr Biol* 12, 93-9. (1995)
69. A. Nahmen von, A. Post, H. J. Galla and M. Sieber: The phase behavior of lipid monolayers containing pulmonary surfactant protein C studied by fluorescence light microscopy, *Eur Biophys J* 26, 359-69. (1997)
70. A. K. Panda, A. Hune, K. Nag, R. R. Harbottle and N. O. Petersen: Structural alterations of phospholipid film domain morphology induced by cholesterol, *Indian J Biochem Biophys* 40, 114-121 (2003)
71. B. M. Discher, K. M. Maloney, D. W. Grainger and S. B. Hall: Effect of neutral lipids on coexisting phases in monolayers of pulmonary surfactant, *Biophys Chem* 101-102, 333-45. (2002)
72. D. Knebel, M. Sieber, R. Reichelt, H. J. Galla and M. Amrein: Scanning force microscopy at the air-water interface of an air bubble coated with pulmonary surfactant, *Biophys J* 82, 474-80. (2002)
73. S. Schurch, M. Geiser, M. M. Lee and P. Gehr: Particles at the airway interfaces of the lung, *Colloid Surf B-Biointerfaces* 15, 339-353 (1999)
74. T. K. Vanderlick and H. Moehwald: Mode Selection and Shape Transitions of Phospholipid Monolayer Domains, *Journal of Physical Chemistry* 94, 886-890 (1990)
75. W. M. Heckl, D. A. Cadenhead and H. Moehwald: Cholesterol Concentration Dependence of Quasi-Crystalline Domains in Mixed Monolayers of the Cholesterol-Dimyristoylphosphatidic Acid System, *Langmuir* 4, 1352-1358 (1988)
76. A. G. Bailey, A. H. Hashish and T. J. Williams: Drug delivery by inhalation of charged particles, *J Electrostat* 44, 3-10 (1998)

Electrical surface potential of pulmonary surfactant

77. P. Brand, I. Friemel, T. Meyer, H. Schulz, J. Heyder and K. Haussinger: Total deposition of therapeutic particles during spontaneous and controlled inhalations, *J Pharm Sci* 89, 724-731 (2000)

78. H. T. Robertson, W. A. Altemeier and R. W. Glenny: Physiological implications of the fractal distribution of ventilation and perfusion in the lung, *Ann Biomed Eng* 28, 1028-31. (2000)

79. A. Tsuda, R. A. Rogers, P. E. Hydon and J. P. Butler: Chaotic mixing deep in the lung, *Proc Natl Acad Sci U S A* 99, 10173-8. (2002)

Abbreviations: KPFM: Kelvin probe force microscopy; DPPC: dipalmitoyl phosphatidyl choline; AFM: atomic force microscopy

Key Words: Lipid Biophysics, Atomic Force Microscopy, Kelvin Probe Force Microscopy, Electrical Surface Potential, Pulmonary Surfactant, Surfactant Associated Protein C, Review

Send correspondence to: Matthias Amrein, Department of Cell Biology and Anatomy, Faculty of Medicine, University of Calgary, 3330 Hospital Drive NW, T2N 4N1, Alberta, Canada, Tel: 403-210-8177, E-mail: mamrein@ucalgary.ca

<http://www.bioscience.org/current/vol14.htm>